Analyzing the Spectrum of Stable Single-Bubble Sonoluminescence with Band-Pass Spectroscopy

ABSTRACT

In this paper we investigate the mechanisms responsible for the phenomenon of sonoluminescence (SL) by analyzing the spectrum of stable single-bubble sonoluminescence (SBSL) with band-pass spectroscopy. We describe the methods we used to generate SBSL in a lab setting and the process by which we would collect and analyze data. Due to the unforeseen circumstances of COVID-19 we were forced to change our data analysis and objective of our research. Our new aim was to quantitatively describe the photoluminescent (PL) emissions for DBP doping concentrations of 0.5%, 1%, 2%, 4%, 6%, and a phosphorescent organic light emitting diode (Ph-OLED). We did this by converting the given spectrum to the 1931 International Commission on Illumination (CIE) xy chromaticity coordinates and plotting the coordinates on the CIE chromaticity diagram. This gave us a numerical indication of the color of the emitted light. We found that the PL emissions were in the red-orange color range while the Ph-OLED emission was light green. With the skills we gained from analyzing the PL spectra, we have the ability to do the same analysis on the spectrum we would obtain from SL. Determining the chromaticity coordinates of the SL emissions would allow us to further investigate the mechanisms responsible for SL.

KEY WORDS: Sonoluminescence, Bubble, Emission, Photomultiplier Tubes, Spectroscopy

INTRODUCTION

Sonoluminescence is a physical process by which sound waves are turned into light and heat. This phenomenon was discovered in the 20th century, but it wasn't until recently that the interest in sonoluminescence peaked in the scientific community due to its implications on the field of sonochemistry which uses the high internal temperatures of SBSL for the fabrication of nanomaterials. There are questions as to the mechanism responsible for the light emission of SBSL, but the most plausible explanations can be classified as either thermal or electrical processes. In our research, we were given the data and figures of the spectra of the emitted light from SBSL. If an electrical process were responsible for the emission of light, we would have observed strong spectral lines. If a thermal process was responsible for the emission of the light, the obtained spectrum would have matched the form of blackbody radiation. From here we could use the blackbody temperature to determine the internal temperature of the bubble before collapse.

Unfortunately, COVID-19 prevented us from continuing on this path of research. Instead, we were given PL spectra for DBP doping concentrations of 0.5%, 1%, 2%, 4%, 6%, and a Ph-OLED. We aimed to quantitatively describe the color of these emissions. To do this, we converted the spectral power distribution of the light to the 1931 CIE xy chromaticity coordinates. The CIE chromaticity coordinates give a uniform indication of the quality visible light independent of brightness. Converting the power distribution of the emitted light allowed us to determine the color of the emitted light based on its wavelength and intensity.

There are various motivations for the research of sonoluminescence. The majority of these motivations stem from the desire to better understand the phenomenon and uncover its practical uses. Single-bubble sonoluminescence is considered to be the most efficient energy focusing mechanism in physics [1] producing energies as high as 12 orders of magnitude. This efficient energy focusing can be used across a wide range of fields. There are research efforts to use the phenomenon for the dissolution of physical samples, to use it for industrial and medical shock waves, to further the field of sonochemistry for the production of nanomaterials, to use it as a catalyst for nuclear fusion, and more.

METHODOLOGY

In this experiment, a stable, single bubble was isolated in a container of deoxygenized water. A standing acoustic wave was then produced as a signal generator and an amplifier were connected together with two piezoelectric crystals which behaved as speakers transmitting the sound wave into the deoxygenized water. An oscilloscope along with a third piezoelectric crystal were used as a microphone to read the output sound. The single bubble in the water was then suspended at the antinode of the standing wave and driven at the resonant frequency
of the container. The wave's interaction with the bubble and the deoxygenized water initiated a cyclic process in which the bubble collapsed when the pressure was increased and then reformed when the pressure decreased. Flashes of light were emitted each time the bubble collapsed.

Figure 1 below illustrates the experimental setup used to capture the emitted light. The light passed through a lens and a series of optical filters before being collected by a photomultiplier tube (PMT) which allows for the detection of faint optical signals from weakly emitting sources such as the SBSL. The photodetector converted the light into measurable data with the help of a lock-in amplifier which filtered out as much noise as possible. From here, the spectral lines were able to be observed and analyzed. The spectral lines indicated the wavelength and intensity of the emitted light and the intensity of the emitted light at each wavelength was used to estimate the internal temperature of the bubble before its collapse.

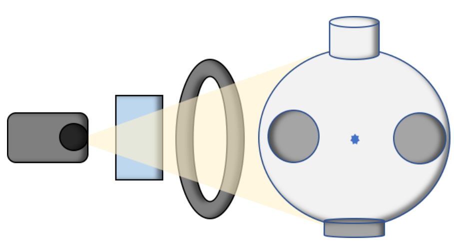

Figure 1: Mockup of the components used for data acquisition: PMT, filter, lens, resonator (left to right)

ANALYSIS

Curves for photoluminescence intensity vs wavelength were plotted for PL intensities of 0.5, 1.0, 2.0, 4.0 and 6.0% transmittance as well as a curve for the phosphorescent organic light emitting diode (Ph-OLED) PL spectrum. We then converted the spectra to the color-mapping functions, the tristimulus values and finally the 1931 CIE xy chromaticity coordinates.

The CIE color-mapping functions are the numerical description of the chromatic response of the "standard observer" defined to represent an average human's chromatic response within a 2° arc inside the fovea. The graphical display of the color matching functions is given in figure 2 below.

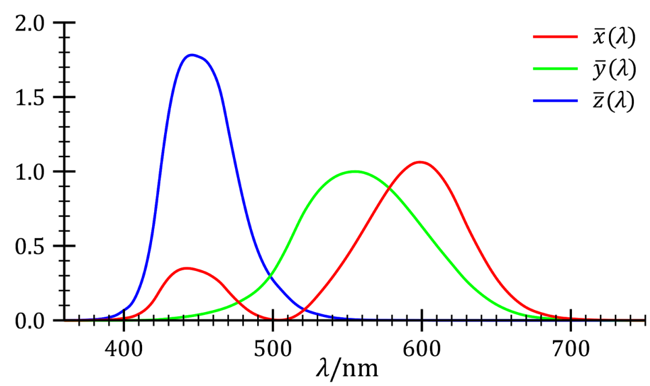

Figure 2: The color mapping function showing the red, green and blue components of light as a function of λ

The CIE color matching functions can be written as a sum of gaussian functions as follows: Let $g(x)$ be a gaussian function defined by

$$g(x; \alpha, \mu, \sigma_1, \sigma_2) = \alpha\, exp(\ (x-\mu)^2/(-2\sigma^2)\ )\ ,$$

where $\sigma = \sigma_1$ for $x < \mu$ and $\sigma = \sigma_2$ for $x \geq \mu$. With the wavelength λ measured in angstroms, the color matching functions are approximated as follows:

$$\bar{x}(\lambda) = g(\lambda; 1.056, 5998, 379, 310) + g(\lambda; 0.362, 4420, 160, 267) + g(\lambda; -0.065, 5011, 204, 262),$$

$$\bar{y}(\lambda) = g(\lambda; 0.821, 5688, 469, 405) + g(\lambda; 0.286, 5309, 163, 311),$$
$$\bar{z}(\lambda) = g(\lambda; 1.217, 4370, 118, 360) + g(\lambda; 0.681, 4590, 260, 138).$$

From here, we calculate the tristimulus values, X, Y, Z, by integrating over the product of the color matching functions, $\bar{x}(\lambda)$, $\bar{y}(\lambda)$, $\bar{z}(\lambda)$ and the spectral power distribution, p, such that

$$X = \int p\, \bar{x}(\lambda)\, d\lambda, \; Y = \int p\, \bar{y}(\lambda)\, d\lambda, \; Z = \int p\, \bar{z}(\lambda)\, d\lambda.$$

The tristimulus values form the CIE XYZ color space which encompasses all color sensations visible to a person with average eyesight. The XYZ color space serves as a standard reference from which many other color spaces are defined. The CIE model defines the value of Y to be the luminance of the light source, while the Z is quasi-equal to blue, and the X is a nonnegative mix of response curves to the other two variables.

The tristimulus values can then be used to obtain the CIE xy coordinates by taking the weighted averages of the tristimulus values as follows:

$$x = X/(X+Y+Z), \; y = Y/(X+Y+Z)$$

These xy values are coordinates for the CIE chromaticity diagram which indicate the color of the emitted light.

RESULTS

The normalized PL spectra we were given to analyze are displayed in figure 3 below. The spectrum is drawn for each of the doping percentages.

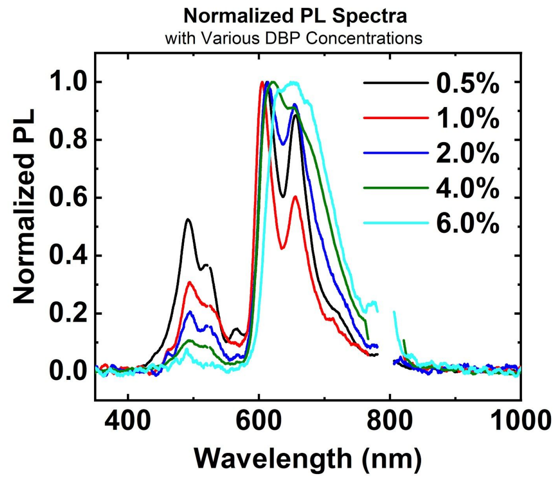

Figure 3: The spectra given for analysis

From the given spectra, we calculated the CIE coordinates and plotted them on the CIE chromaticity diagram below (figure 4).

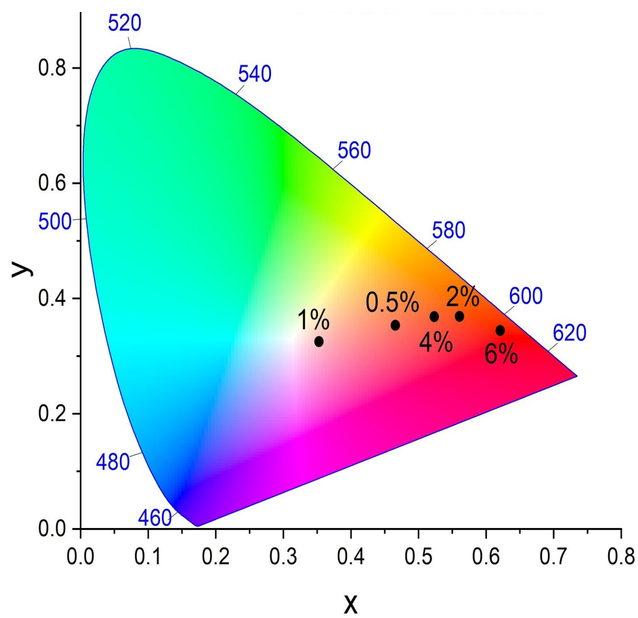

Figure 4: CIE diagram indicating emission colors

The PL emissions were all in the red/orange/pink area of the color map. The lower dopant percentages seemed to emit a lighter shade of color than the higher dopant percentages.

The normalized PL spectrum for the Ph-OLED is displayed below in figure 5. It is apparent that the Ph-OLED has a peak wavelength lower than that of emissions at different dopant percentages.

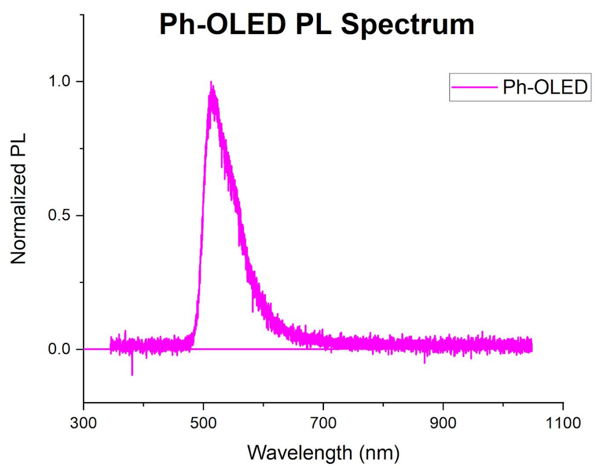

Figure 5: Normalized PL spectrum for Ph-OLED

Following the same procedure of calculating and plotting the CIE xy coordinates resulted in the color map for the Ph-OLED given below. This color map indicates that the Ph-OLED emitted green light.

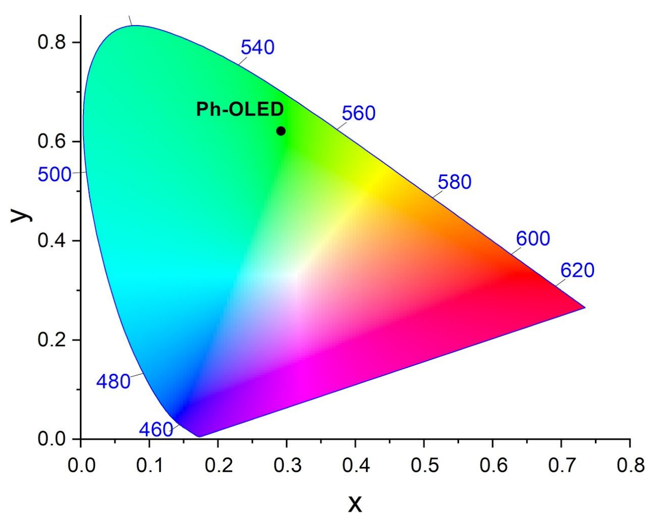

Figure 6: Ph-OLED emissions are light green in color

The specific values for the CIE xy coordinates that we calculated are displayed in the table below. The biggest outlier in the table is the y-value for the Ph-OLED as it is almost twice as large as any of the other calculated y-values. The drastic difference in this y-value is due to the drastic difference in the color of the emission. The Ph-OLED emitted green light while all the other spectra correspond with red light emissions.

Dopant %	CIE x	CIE y
0.5%	0.46574	0.35349
1%	0.35259	0.3253
2%	0.56057	0.3691
4%	0.52328	0.36855
6%	0.62086	0.3445
Ph-OLED	0.29168	0.62151

Table 1: calculated CIE xy values

Our analysis allowed us to take raw data of the PL emissions and determine the color of the emissions. We found that the color of the emitted light generally corresponded with the peak wavelength in the PL spectrum. Whatever the peak wavelength was, its color in the visible light spectrum agreed with the color indicated by the CIE color diagram.

CONCLUSION

With the discussion and figures shown above, we can see that the color mapping functions are useful for finding the spectrum of PL as well as SL. From our photoluminescence data, we determined the emitted color of the PL spectrum which is otherwise difficult to know from the spectra alone. This technique can be extended to many optical experiments, allowing researchers to accurately determine the emitted color.

[1]S. J. Putterman, Sci. Am. **272,** 46 (1995).

[2]R. A. Hiller and B. P. Barber, Sci. Am. **272,** 96 (1995).

[3]S. Baniya, Z.Pang, D. Sun, T. Basel, Y. Zhai, O. Kwon H. Choi and Z. V. Vardeny, SPIE **9941,** 99410H-1 (2016).